Study on Pollutants Formation under Knocking Combustion Conditions using an Optical Single Cylinder SI Research Engine

Apostolos Karvountzis-Kontakiotis[1,2,*], Hassan Vafamehr[1], Alasdair Cairns[3], Mark Peckham[4]

1. Brunel University London, Department of Mechanical, Aerospace & Civil Engineering, CAPF – Centre of Advanced Powertrain and Fuels, Uxbridge, UB8 3PH, United Kingdom

2. City University London, School of Mathematics, Computer Science and Engineering, Northampton Square, London EC1V 0HB, United Kingdom

3. Faculty of Engineering, University of Nottingham, University Park, Nottingham NG7 2RD, United Kingdom

4. Cambustion Ltd., 347 Cherry Hinton Road, Cambridge CB1 8DH, United Kingdom

* Corresponding author email: a.karvountzis@brunel.ac.uk

Abstract

The aim of this experimental study is to investigate the pollutants formation and cyclic emission variability under knocking combustion conditions. A great number of studies extensively describe the phenomenon of knock and its combustion characteristics as well as the effect of knock on engine performance; however the impact of knocking combustion on pollutants formation and how it affects cyclic emission variability has not been previously explored. In this study, an optical single cylinder SI research engine and fast response analyzers were employed to experimentally correlate knocking combustion characteristics with cyclic resolved emissions from cycle to cycle. High-speed natural light photography imaging and simultaneous in-cylinder pressure measurements were obtained from the optical research engine to interpret emissions formation under knocking combustion. The test protocol included the investigation of the effect of various engine parameters such as ignition timing and mixture air/fuel ratio on knocking combustion and pollutant formation. Results showed that at stoichiometric conditions by advancing spark timing from MBT to knock intensity equal to 6 bar, instantaneous NO and HC emissions are increased by up to 60% compared to the MBT operating conditions. A further increase of knock intensity at the limits of pre-ignition region was found to significantly drop NO emissions. Conversely, it was found that when knocking combustion occurs at lean conditions, NO emissions are enhanced as knock intensity is increased.

Keywords: knocking combustion, cycle resolved emissions, NO formation, optical research engine, cyclic emission variability

Highlights

- Experimental investigation of knocking combustion and cycle resolved emissions.
- Effect of knock index on NO formation.
- Utilization of instantaneous flame images to interpret emissions formation.
- Effect of knock and heavy knock conditions on cyclic emission variability.

Nomenclature

Acronyms			
ATDC	After Top Dead Centre	imep	Indicated mean effective pressure
Bmep	break mean effective pressure	KI	Knock Intensity
BTDC	Before Top Dead Centre	MBT	Maximum Breaking Torque
CCV	Cyclic Combustion Variability	NO	Nitric Oxide
CEV	Cyclic Emission Variability	SI	Spark Ignition
COV	Coefficient of Variation	TDC	Top Dead Centre
HC	Hydrocarbons	λ	Air/fuel equivalence ratio

1 Introduction

Gasoline engine technology has entered one of the most exciting periods in its long history: downsizing, hybridization and stricter emission standards determine the future of SI engines [1]. Advanced engine requirements for high power density and low fuel consumption can be achieved through high boost, direct injection, engine start&stop [2] and lean burn operation. Implementation of this technology in SI engines increases the potential possibility that under certain operating conditions auto-ignition or pre-ignition can occur [3]. Knock not only limits engine thermal efficiency but it also affects the formed emissions during combustion. As pollutants formation is directly linked to the combustion process, it is critical to understand the effect of abnormal combustion cycles on emissions performance and variability. To this end, meeting fuel economy requirements and future emission standards in high-efficiency SI engines requires a well understanding of knock and its effect on engine emissions.

Knock is as old as SI engine itself [4] and takes its name from the metallic 'pinging' noise that auto-ignition (spontaneous combustion) creates before the piston reaches TDC. Knock can be divided into two main groups: light to medium knock and super knock. Light to medium knock limits compression ratio and as a consequent the engine thermal efficiency due to the end-gas auto-ignition. Auto-ignition is the fast discharge of chemical energy contained in the end-gas, which is the final fraction of the air-fuel mixture that enters the cylinder but without inclusion into the flame front reaction [5], [6]. On the other hand, super knock limits raising the boost pressure and the engine power density due to detonation, also known as pre-ignition [7], [8]. Pre-ignition occurs earlier to auto-ignition and leads to a fast and violent combustion that can potentially damage the engine. Apart of the great number of studies on knocking combustion, the correlation between knock intensity, heat transfer, fuel chemistry, pressure oscillations and oil droplets is not well understood [3]. Nowadays, the main research focuses on super knock due to the high boost technology applied in high power density downsized engines, which usually occurs under low speed and high load engine operating conditions.

Fuel and cylinder charge properties as well as engine calibration can affect combustion characteristics and simultaneously affect the formed emissions. Methods for suppressing engine knock and controlling emissions involve the optimization of those parameters. Conventional suppression methods of engine knock include control strategies for retarding spark timing [9], raising fuel octane number by using additives [10], [11] and enriching mixture [12] when knock occurs. Recent studies correlated the effect of cooled EGR with the reduction of knocked cycles and fuel consumption. Diana et al. presented a knock free operation of a stoichiometric SI engine at full load conditions with a compression ratio of 12.5 by using cooled EGR [5]. Same trend was also observed in another experimental study where it was shown that the resistance to knock is strongly increased by cooled EGR [13]. It was also found that utilization of EGR can significantly reduce emissions by up to 90% [5], [14], [15], while HC emissions increase across the EGR range [16], [17]. Air-fuel ratio can also affect engine knock limit. Although leaner mixtures benefit fuel consumption, retarded combustion is required to avoid knock [6], while over-fuelling increases the knock limits of the engine [18]. In another study, it is reported that the EGR and the lean burn operation exhibit lower average knock indexes. Due to the longer combustion duration by utilizing EGR and lean burn, heat transfer is enhanced and end-gas temperature is decreased [19]. Conversely, another experimental work using a single cylinder research engine that was supplied with ON 75 proved that lean mixtures have the earliest onset of knock, and the highest knock intensity [20]. Furthermore it was noted that lean mixtures are particularly sensitive to the charge heating during compression. Overall, this research implies that excess air at high loads does not suppress knock.

More than 700 research studies exist in literature on the research area of engine knock [3]. The main research studies that deal with engine knock can be categorized on knock detection, numerical simulation, optical diagnostics, theoretical studies, engine optimization and fuel/oil properties. Although knocking combustion can significantly affect formed emissions, the effect of knocking combustion on pollutants formation is at an even earlier research stage and there is a significant lack of studies in this research field.

Pollutants formation during engine combustion is correlated both with mixture properties such as air/fuel ratio, residual gas fraction and fuel properties and with the combustion type. At normal combustion conditions (deflagration), NOx formation is primarily controlled by oxygen availability under lean or rich conditions while within the stoichiometric window formed NOx concentration is correlated with the combustion burn rate [21]. Under no knocking combustion, previous studies showed that as in-cylinder peak pressure is increased, NOx emissions are proportionally increased [21]–[23]. However under knocking combustion, the emissions formation mechanism can significantly change. As knock intensity is increased, residence time of the residual gases in the burned zone is significantly decreased and peak temperature can be enhanced. On the one hand, under super knock conditions combustion duration is decreased to less than 2^{o} CA which means that combustion is almost isochoric, post-combustion residence time is significantly lower but peak temperature and pressure are much higher than in normal

SI combustion. Such a type of combustion presents many similarities with HCCI combustion that is known for the ultra-low NOx emissions and the relatively higher CO and HC emissions [24]. On the other hand, under light knock conditions NOx concentration that is formed in the post-flame zone during normal combustion is expected to be increased due to the high temperatures of end gas auto-ignition. However, the above described trends have not been explored in literature and more research is required to well understand the relationship between pollutants formation and knock index.

A great number of research studies investigate the main mechanisms of pollutants formation, described in detailed elsewhere [25]. The most well-known NOx formation mechanism is the thermal one, co-called as extended Zeldovich mechanism which is responsible for the majority of the formed NO in the post flame gas zone [26], [27]. Apart from the thermal mechanism, the prompt NO mechanism [28] can be significant at stoichiometric and richer mixtures [29], [30], the N_2H mechanism becomes important at slightly rich conditions [31] and finally the N_2O chemical pathway appears at slightly lean conditions [26], [32]. Regarding carbon monoxide, CO formation is mainly kinetically controlled by water gas shift reaction [33]. Finally, hydrocarbons (HC) are the consequence of incomplete combustion of hydrocarbon fuel [34]. In most studies, simplified chemical mechanisms are utilized to predict pollutants formation [29], [35]. Recently, Karvountzis et al. [36], [37] proposed the use of a detailed chemical kinetics model to predict pollutants formation in an SI engine, which operates in the post-combustion zone. The latter is the most accurate state-of-the art emission model existing in literature, as the validation against experimental cycle resolved emission values for both NO and CO emissions under various engine operating conditions showed errors less than 10% and compared to simplified emissions models improvements were higher than 50% [38]. However the accuracy of this emission model under knocking conditions has not been explored, due to the lack of experimental data.

Although the relationships between combustion characteristics and pollutant formation under normal combustion have been explored in the past, the effect of knocking combustion on pollutants formation is not well understood. Few studies in the past presented an engine model that can predict knock limit and NOx emissions [39], [40], [41]; however those models do not present the pollutant formation under knocking combustion conditions. The only known relationship is that knock results to an increase in CO and HC emissions due to incomplete combustion [42]. Furthermore, there is a lack of experimental data at this research field, as there are no experimental studies presenting the correlations between knock index and emissions performance on a cycle to cycle base. Simultaneously, the effect of pressure oscillations and hot spots (occurring during knocking combustion) on pollutants formation is also unknown. In the past, fast response analyzers were successfully employed to measure cyclic emission variability under normal combustion conditions [43]. Optical diagnostics have been also utilized to deeper understand the end gas auto-ignition mechanism and explore the detonation limits at pre-ignitive cycles [7]. However, as authors are aware, a study that employs both fast response analyzers to detect emissions from cycle to cycle and optical diagnostics to correlate combustion characteristics with cycle resolved emissions doesn't not exist in literature.

This experimental work studies the correlation between pollutants formation and knock index, primarily NO and HC, under various air-fuel ratio and spark ignition timings using an optical single cylinder SI engine. Fast response analyzers were employed to measure the cycle resolved NO and HC emissions. Images of the visible light from combustion heat were captured through an overhead window using a high speed camera. The aim of this study is to give insights between the type of combustion (deflagration, end gas auto-ignition and detonation) and the formed emissions and determine by which extent emissions are increased under knock. The output of this study can be applicable to new engine design requirements for more efficient and less pollute SI engines. To the best knowledge of the authors, this is a unique study of its kind.

2 Experimental Setup

2.1 Optical Engine

A customized single cylinder research engine with a distinct optical arrangement was employed in this study [18], [44], [45]. The basic engine characteristics of the engine are presented in **Table *1***. The bottom-end of the engine is based on a commercial Lister-Petter TSI with a combined full-bore overhead access and a semi-traditional poppet-valve valvetrain. Due to the full-bore overhead optical access, the glass of the engine head was designed to withstand peak combustion pressures up to 150bar. The engine incorporates a flat piston crown, two inlet ports, and originally was designed with two exhaust ports. As the purpose of this study is focused on knocking combustion, one of the exhaust valves was deactivated in order to assist end-gas autoignition, by increasing residual gas fraction [46]. A schematic presentation of the optical cylinder head is illustrated in **Figure *1***. The recessed side mounted poppet valves guaranteed valve overlap without piston clash and to maintain a compression ratio of 8.4:1 [45]. Last but not least, the research engine was coupled to an eddy-current dynamometer with a maximum power absorption/supply of 10kW.

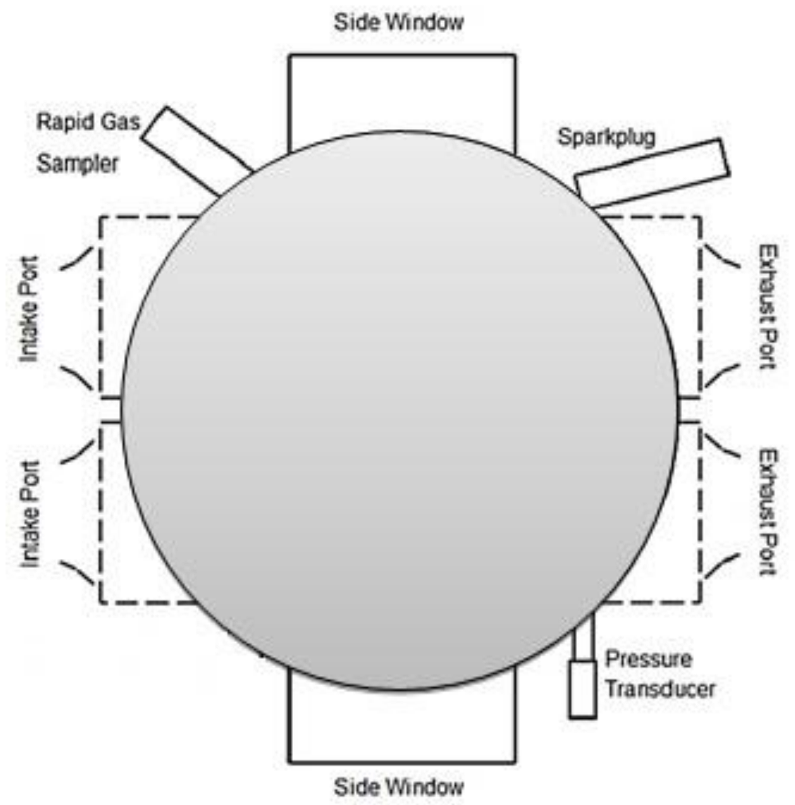

Figure 1: Schematic presentation of the optical engine cylinder head [18].

Table 1: Engine characteristics of the optical single cylinder research engine.

Parameter (unit)	**Value**
Number of Cylinders (-)	1
Compression Ratio (-)	8.4:1
Stroke (mm)	89
Bore (mm)	95
Displacement (cc)	631
Con-rod Length (mm)	165.16
Valve Lift (mm)	5
Inlet Valve Openings/Closing (°BTDC)	375/145
Exhaust Valve opening/Closing (°ATDC)	120/350

The engine fuel supply was regulated by a Bosch EV6 PFI fuel injector operating at 3 bar rail pressure. The PFI injector had a 2-hole pattern forming a dual plume spray pattern targeted toward the intake valves. The injection timing was fixed at 400° BTDC firing under all operating conditions. The fuel used in these tests is PRF75, as a result of blending isooctane and n-heptane (provided by a chemical supplier) on a volumetric basis in small batches immediately prior to each testing session. The chemical properties of the reference fuels are provided in **Table *2***. The ignition system consisted of an NGK ER9EH 8mm spark plug supplied by a Bosch P100T ignition coil.

Table 2: Fuel properties

Property	**Iso-Octane**	**n-Heptane**
Chemical Formula	C8H18	C7H16
Boiling point at 1 atm (°c)	99.2	98.4
Enthalpy of vaporisation at 298.15 K (MJ/Kmol)	35.14	36.63
Density at 25°C (Kg/m^3)	690.4	681.5
Latent Heat of Vaporisation(kJ/kg)	308	318
Reid Vapour Pressure (bar)	0.52	0.12
Oxygen Content by Weight (%)	0	0
Volumetric Energy Content (MJ/l)	30.6	30.48
RON (MON)	100 (100)	0 (0)

2.2 Experimental Configuration and Measurements

Experiments were conducted using the experimental setup schematically illustrated in **Figure *2***, while the main specifications of the relevant components are presented in **Table *3***. The test protocol included the recording of high frequency data, low frequency data and natural light photography data. The high frequency data were recorded in a National Instruments (NI) data acquisition card and included the in-cylinder pressure, encoder crankangle signal, exhaust temperature and exhaust NO and HC emissions recordings from the fast response analyzers. The low sampling frequency data comprised ECU derived signals, including air/fuel ratio value (λ sensor), ignition timing, throttle position, inlet air pressure and temperature and coolant temperature. Recording also included the high frequency photography data of the combustion evolution. Finally, the three (3) set of data are stored in a computer as it is illustrated in **Figure *2***.

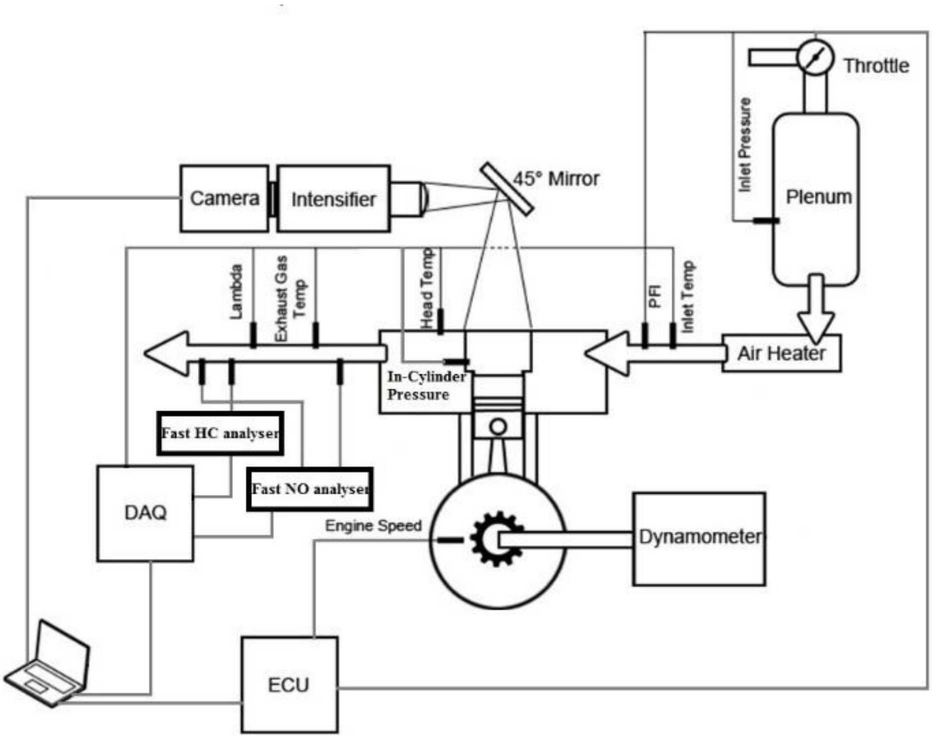

Figure 2: Schematic illustration of the experimental configuration.

An AVL GH14DK pressure transducer was implemented on the side of the exhaust valves to measure cylinder pressure (**Figure *1***). It was manufactured to fit this particular handmade engine cylinder head and its position was at the region where autoignition usually takes place. It has to be mentioned that when knock occurs, pressure distribution across the combustion chamber is not uniform and the location of the transducer can affect the recordings [47]. The signal from the transducer was fed to an AVL Flexifem charge amplifier. The error in the cylinder pressure measurement was less than ±1% full scale reading (FSO). The exhaust gas temperature was measured with a K-type thermocouple connected to the relevant transducer, with maximum error of ±0.75% of reading. The response time of the thermocouple was low (0.1sec); therefore the thermocouple was utilized to measure averaged temperature per cycle rather than monitoring exhaust temperature profile. The total experimental rig is presented in **Figure *3***.

Table 3: Main specifications of measurement equipment.

In-cylinder Pressure Sensor: AVL GH14DK	
Pressure range	0-300 bar
Natural Frequency	~ 170 kHz
Linearity	≤±0.3% full scale output (FSO)
Sensitivity Drift	≤±1%
Pressure Sensor Amplifier: AVL Flexifem INDI	
Linearity	≤±0.5% full scale output (FSO)
NO fast response analyzer: Cambustion CLD500	
Response time	NO: 2ms, NOx: 8ms
Linearity	≤±1% full scale output (FSO)
HC fast response analyzer: Cambustion HFR400	
Response time	HC(C1): 4ms
Linearity	≤±1% full scale output (FSO)
Natural Light Photography: Memrecam fx-6000	
Image Resolution	512 × 384 pixels.
Frame Speed	6000 (fps)

Figure 3: The experimental test rig.

High frequency cycle resolved exhaust emissions measurements were conducted using two fast response analyzers from Cambustion Ltd. The Cambustion CLD500 analyzer was employed for the cycle resolved NO emissions. From the two available sampling heads of this analyzer, one was used and installed directly downstream of the exhaust valve of the cylinder, while the second probe was installed downstream enough to the exhaust gases to get an average value of NO emissions. The sampling response time of NO emissions was in the order of 2 ms (**Table *3***). Simultaneously, Cambustion HFR400 analyser was employed for HC measurement. The only used sampling head was installed downstream of the exhaust valves and its sampling time was about 4 ms. Signals from both heads (3 in total) were directed to the NI data acquisition card.

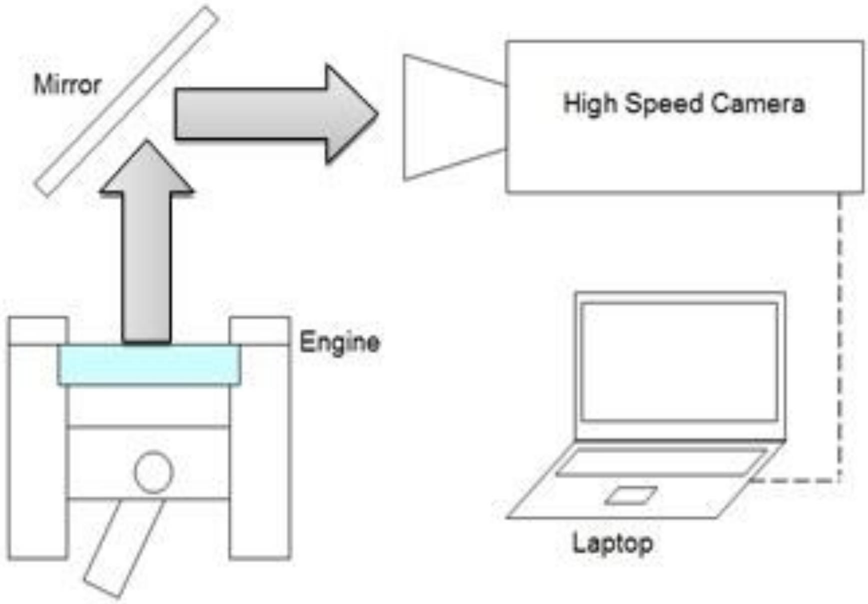

Figure 4: Schematic of experimental setup for combustion imaging

Images of the visible light from combustion heat were captured through an overhead window as shown in **Figure *4***. The camera was capable of imaging at 6000 frames per second (fps) with a resolution of 512 x 384 pixels. All cycles presented in this paper were imaged at 6000fps with an exposure time of 167µs. The internal memory of the camera allowed for a total of 10,000 frames to be recorded before the data were stored in a hard drive (laptop). At 1200rpm this allowed for 16 cycles to be recorded in a single test. Due to the large variation in intensity of the light emission from combustion between cycles, the gain was adjusted for each cycle to improve the clarity of the images.

The reason that in this study an optical engine has been employed is to qualitatively explain the cyclic resolved emission values under various knocking conditions by utilizing optical data. Realistic results from commercial engines may quantitatively change, as explained elsewhere [44].

2.3 Engine Test Protocol

A fixed reference point was obtained by running the engine under normal non-knocking part-load operation until the cylinder head metal temperature reached 88°C. At this temperature knock was induced by resetting the spark timing. After capturing the data, the engine was stopped and allowed to cool down before the process repeated. This process kept the measured wall temperatures within a small range (<5°C peak-to-peak variation), which was considered necessary when considering knock in a qualitative manner with an engine setup lacking water cooling in the head. The thermodynamic results were averaged over three sets of 100 cycles for each test condition. The sump oil temperature remained moderately low throughout testing (~40°C). **Table *4*** shows the engine test conditions.

Table 4: Engine operating conditions.

Parameter (unit)	Value
Engine Speed (RPM)	1200±5
Relative AFR (λ)	1±0.01
Inlet Pressure (bar)	0.9±0.02
Inlet Air Temperature (°C)	66±2
Exhaust Bridge Temperature (°C)	130±2
Head Temperature (°C)	88±1

2.4 Data Processing

An example of processing the in-cylinder pressure of two consecutive cycles with KI index 0.76 bar (light knock cycle) and 15.1 bar (super knock cycle) respectively versus NO concentration is given with reference to **Figure *5***. During the valve-closed part of the current cycle, the analyzer measures the NO level of the gas remained in the exhaust manifold from the previous cycle. When exhaust valve opens (EVO) a portion of the (in-cylinder) gas violently exits the cylinder (blow-down) and clears the exhaust manifold from the previous cycle gas. However, a delay between EVO and analyzer response (point A in **Figure *5***) is observed, attributed to the distance between the valve outlet and the sampling probe, as well as to the instrument response time [23]. After the exhaust valve closes (EVC), the analyzer signal exhibits a slight fluctuation (area B-C in **Figure *5***), indicating a variation of NO concentration in the cylinder gas. The NO concentration may vary from cycle to cycle due to the combustion process. During the closed part of the next cycle, the analyzer signal can be considered constant (part C-D in **Figure *5***) and corresponds to the NO level of the current cycle. This average value is taken as the NO emissions amplitude of the current cycle. Last but not least, **Figure *5*** also shows that the level of NO (C-D area) after a light knock cycle and after a super knock cycle (C' point) can significantly vary. The deeper understanding of this observation is within the aim of this study. A similar procedure was followed to detect HC concentration at each combustion cycle, taking into account the variations in signal delay, due to the different positioning of the sampling probes for NO and HC species. More details on the exact process per pollutant can be found in open literature [21], [23], [48], [49].

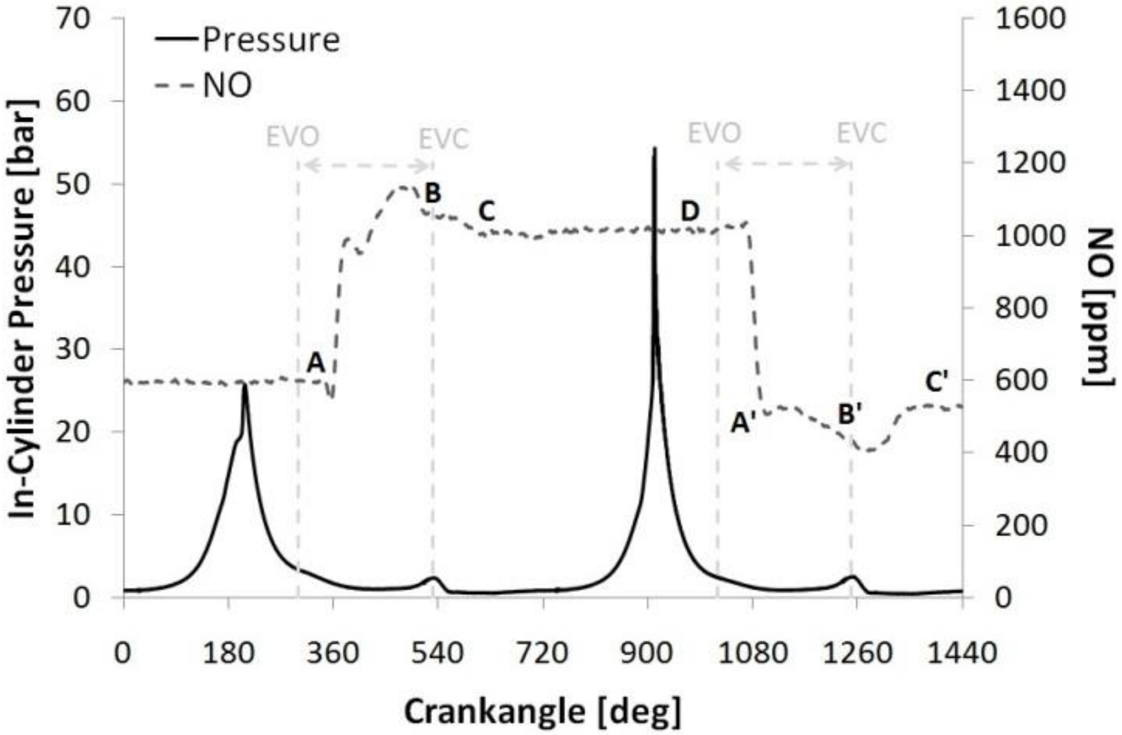

Figure 5: Schematic illustration of the fast NO signal in reference to in-cylinder pressure for two consecutive cycles with KI=0.76 bar and 15.1 bar respectively.

3 Results and Discussion

3.1 Effect of Spark Ignition Timing

The phenomenon of knock is controllable by the spark advance as advancing or retarding the spark timing can increase or decrease the knock severity or intensity respectively [47]. Although knock varies substantially from cycle to cycle and doesn't occur at each combustion cycle, an average combustion cycle can present the 'mean' picture of knock intensity. Various spark timings lead to different heat release rate histories, which can be linked to end-gas pressure and temperature conditions that can cause autoignition. The latter can be observed as a rapid increase in the pressure trace accompanied by fluctuations which amplitude varies with time.

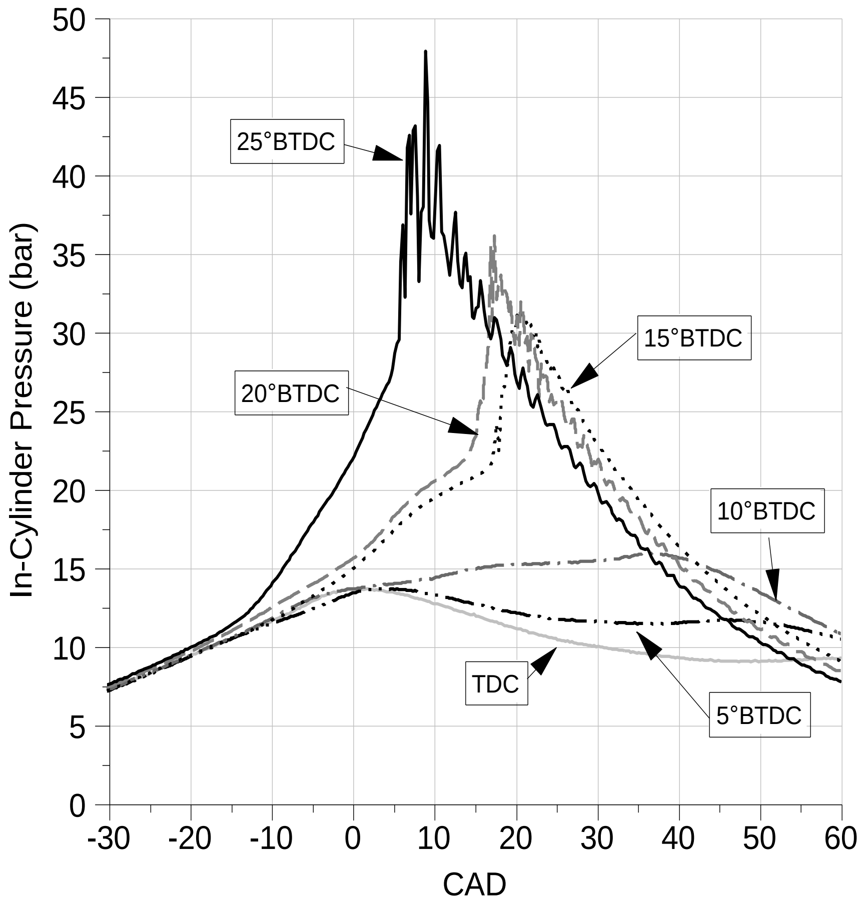

Figure 6: In-cylinder pressure traces for six (6) different ignition timings. Advanced ignition leads to heavy knock.

Figure *6* shows six (6) different combustion cycles where the range of knock intensity varies. The illustrated pressure traces represent the average imep cycle of the measured 300 cycles at each spark timing condition. It is observed that as ignition timing shifts from TDC to 25°

BTDC, the magnitude of peak combustion pressure and the amplitude of pressure fluctuations are impressively increased. In fact, the peak in-cylinder pressure when ignition timing occurs at TDC compared to the ignition timing occurs at 25^{o} BTDC is more than three (3) times higher. Furthermore, it is revealed that knock intensity increases exponentially as knock occurs closer to top center, earlier in the combustion process.

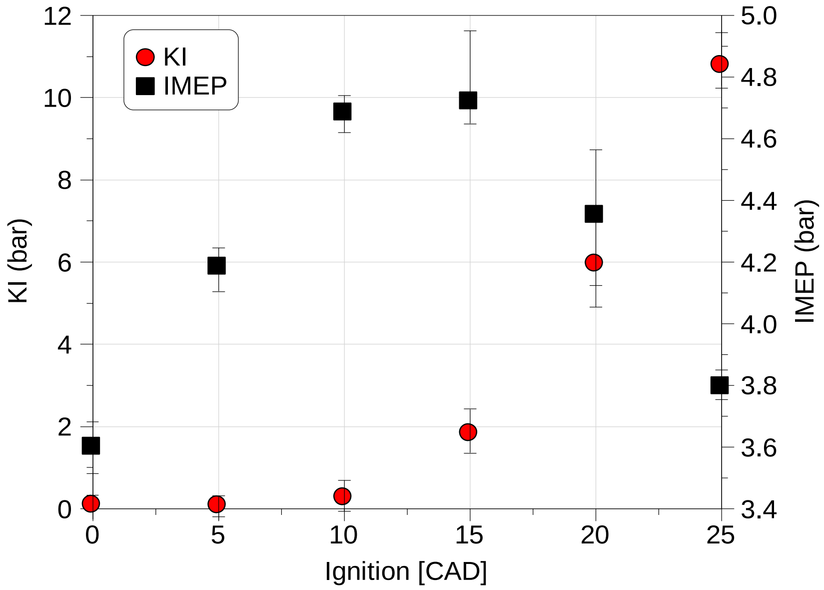

Figure 7: Impact of spark ignition timing on IMEP and KI under stoichiometric conditions and wide open throttle conditions.

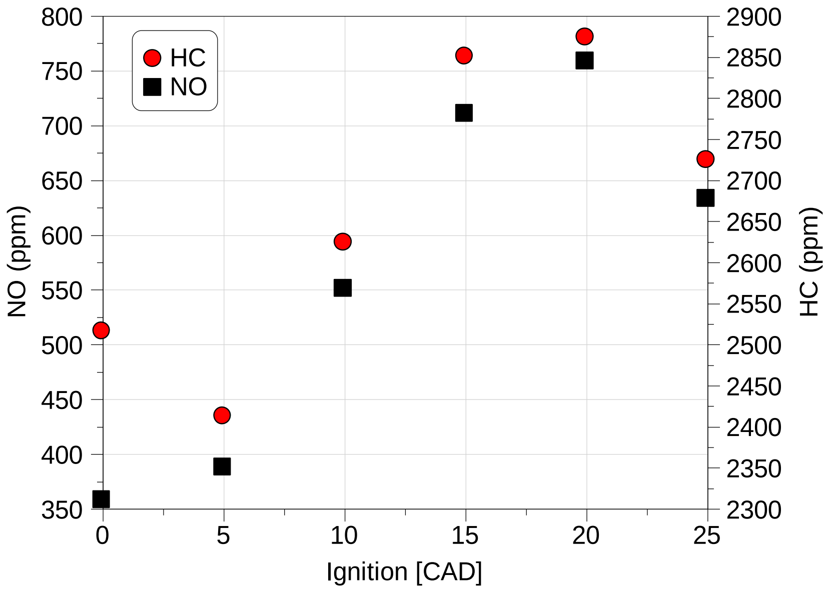

Figure 8: Impact of spark timing on NO and HC emissions, considering mean value.

Pressure traces substantially vary from cycle-to-cycle; therefore mean values of imep and KI as well as the variability of these indexes can explain the transition from normal combustion to heavy knock by advancing spark timing. **Figure *7*** schematically presents the relationship between both KI and imep against spark timing. MBT is achieved at spark timing close to 10^o BTDC, where the mean value of imep is maximized and the COV of imep is minimized. Further spark advance leads to higher imep variability, the mean value of imep drops and KI is exponentially increased. At 15^o BTDC spark timing, KI is equal to 2 bar and can be classified into a medium knock case while further spark advance leads to heavy knock cycles.

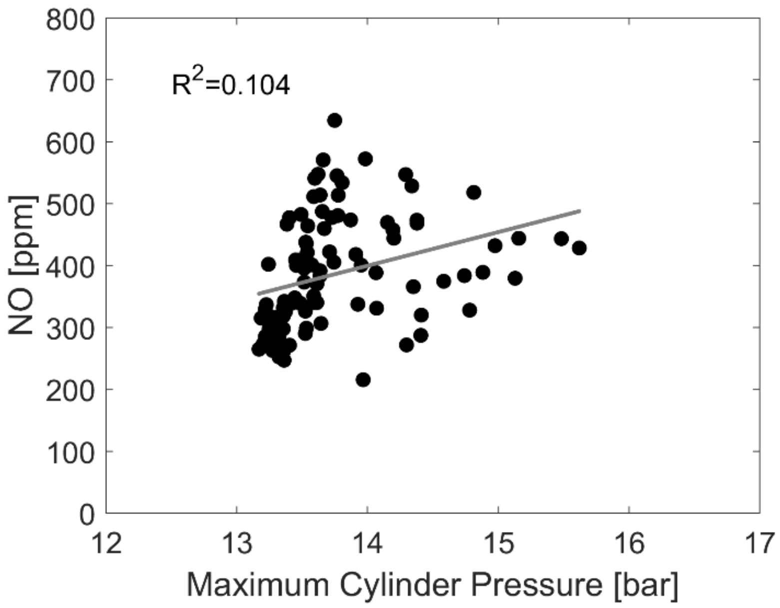

Figure 9: Relationship between maximum cylinder pressure and NO formed emissions under normal combustion conditions (spark timing at 5^o BTDC).

Cycle to cycle variability is recognized as the main reason of cyclic emission variability; however the impact of knocking combustion on pollutants formation has not been previous investigated extensively. The averaged and variation range of the emission values for 300 combustion cycles as well as the relationship between NO and HC emissions against spark timing are illustrated in **Figure *8***. HC are increased against spark timing due to incomplete combustion as KI is increased. However, under heavy knock conditions mean HC are slightly decreased as pre-ignition appears and combustion characteristics change. Regarding NO, it was found that engine-out NO are enhanced versus spark timing which is continued until heavy knock conditions at spark timing 20^o BTDC and then average formed NO is decreased. Previous studies on cyclic NO variability presented that MBT is related with the maximum mean NO value and the minimum COV_{NO} value [43], while the effect of knocking combustion in this relationship is not usually considered. The current tested experimental case clearly presents that knock can further increase mean NO exhaust emissions by up to 36%, while considering NO variability, instantaneously this increment can reach up to 60%. A further analysis to better understand the deeper reason of this trend is needed and followed in this study.

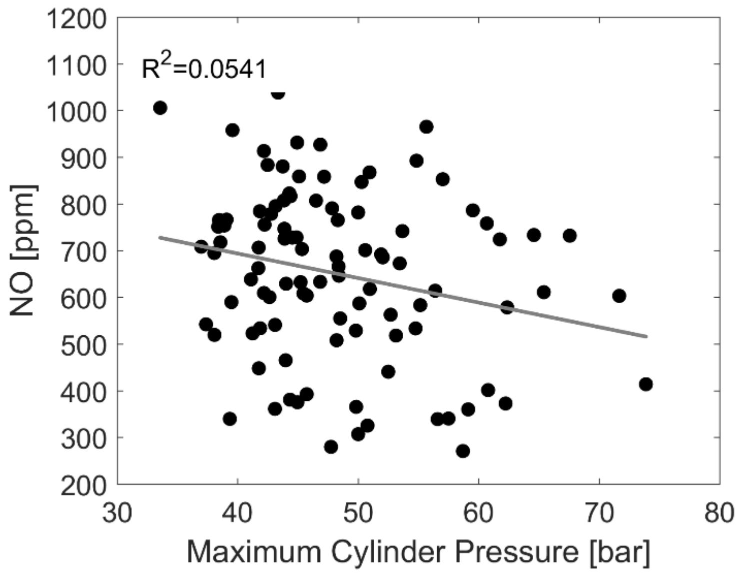

Figure 10: Relationship between maximum cylinder pressure and NO formed emissions under heavy knock conditions (spark timing at 25^o BTDC).

In addition to NO emissions, **Figure *8*** presents the relationship between HC emissions and spark timing. HC emissions mean value is increased as spark ignition timing is advanced apart from the TDC ignition timing point, as this point seems to represent a very late combustion, very slow heat release rate that declares incomplete combustion takes place. In general, HC emissions present similar trend to NO emissions against spark timing. Under knocking conditions (spark timing exceeds 10^o BTDC), HC emissions are enhanced by up to 10% while under heavy knock conditions a slight drop compared to the peak HC emissions is observed.

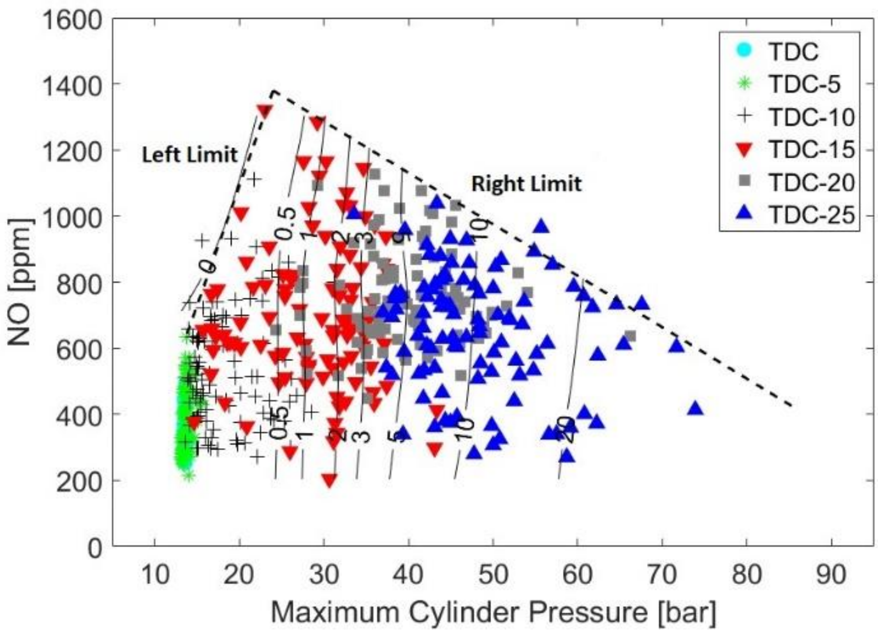

Figure 11: Relationship between maximum cylinder pressure and NO formation for various KI conditions (contour lines) as a result of various ignition timing conditions under stoichiometric conditions.

Nitric oxide is mainly formed at high temperatures, through the well-known extended Zeldovich thermal mechanism [26]. Peak combustion temperature and residence time at high temperature conditions are the two primary reasons on nitrogen oxidation. **Figure *9*** represents the relationship between maximum cylinder pressure and NO emissions for 100 consecutive cycles under normal combustion conditions (ignition timing 5^{o} BTDC). The trend of these points is found close to linear, validating similar observations from previous studies [21], [43], [50]. In fact, deviations from this linear correlation can be related with the cyclic dispersion of mixture parameters such as residual gas fraction, fuel trapped mass or air-fuel ratio at each combustion cycle. This linear trend clearly shows that as maximum cylinder pressure is increased NO formation is enhanced. However a similar analysis of the data under heavy knock conditions (ignition timing 25^{o} BTDC) showed the opposite linear trend; higher maximum cylinder pressure leads to lower NO emissions (**Figure *10***). Furthermore, the dispersion of the points is at much higher range compared to the case of normal combustion conditions. The latter is resulted from the stochastic behaviour of knocking combustion conversely to the more robust normal combustion.

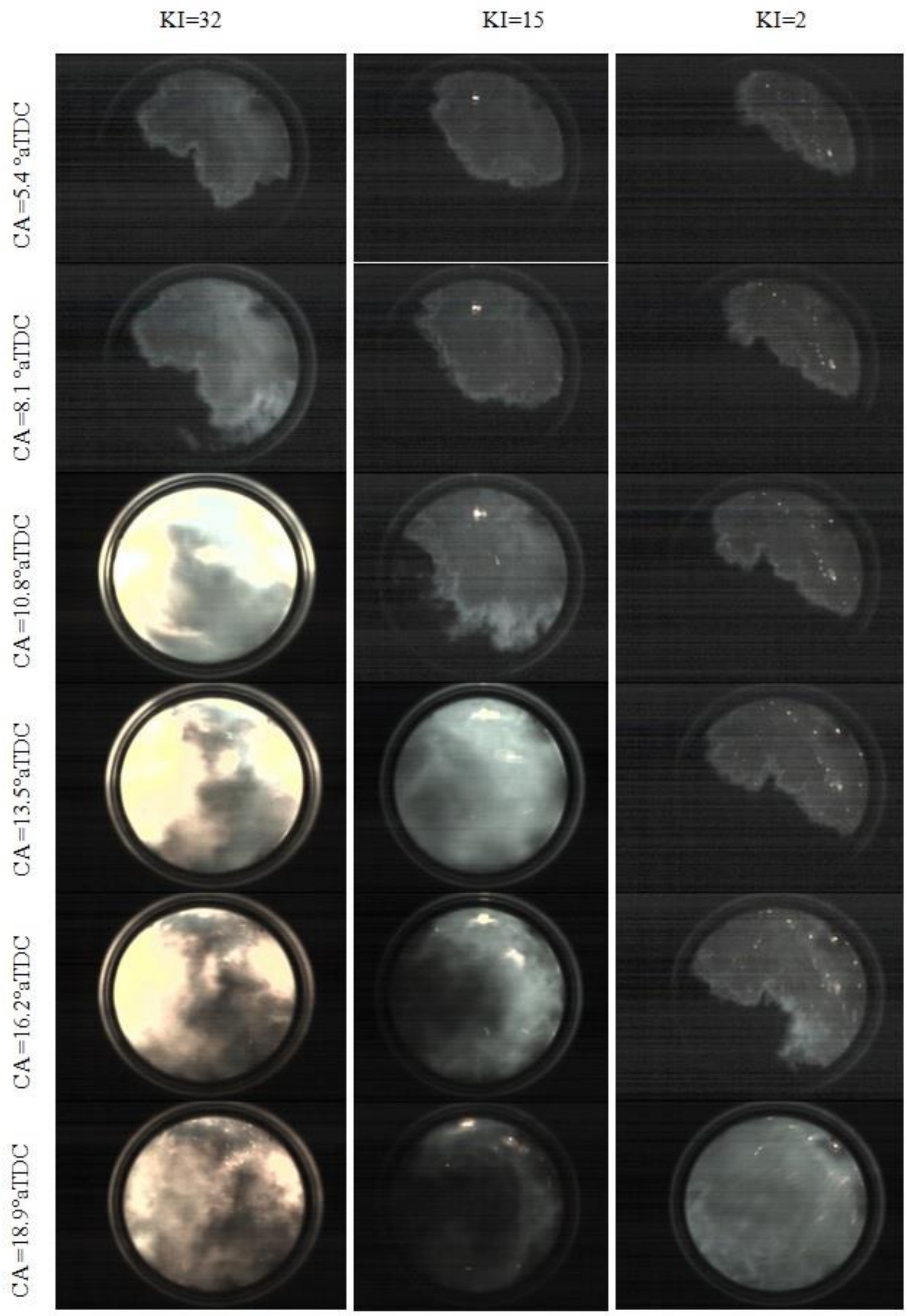

Figure 12: Comparison of various KI conditions.

NO variability is highly related to the combustion rate, as approved elsewhere [38]. **Figure *11*** illustrates the relationship between maximum cylinder pressure and NO emissions for various spark timing conditions. It is observed that the area where points occur is restricted by a 'left' and 'right' limit that both form a triangular region. The third axis of this plot represents the knock intensity which is illustrated as contour lines on the same figure. The 'left' limit of this plot is well-matched with the KI equal to zero contour line. In fact, it describes the observed trend found at **Figure *9***; higher maximum cylinder pressure leads to higher NO emissions under normal SI combustion conditions and it is the limit of NO formation under deflagration conditions. Moving to the right part of **Figure *11***, maximum cylinder pressure increases as end-gas auto-ignition starts to occur. Under knocking combustion condition, it is observed that the variation between maximum and minimum NO emissions at higher maximum cylinder pressure is decreased and reaches a narrow window area at extreme peak in-cylinder pressures. The latter forms the right region limit which is hard to explain from recorded thermodynamic data. Therefore natural light photography data were employed to better understand this trend.

Set out in **Figure *12*** are flame images from three (3) different combustion cycles under various knock intensity conditions; namely light knock, medium knock and heavy knock. It can be seen that for KI=2, auto-ignition is observed at the late phase of the combustion process. Burned zone occurs for long time, enough for the post-flame kinetics to form a substantial amount of NO emissions. On the opposite site, at heavy knock cycles, auto-ignition occurs much earlier and respectively burned zone also occurs less, NO residence time is decreased and although peak temperature is higher final formed NO emissions are significantly lower to normal combustion case. Summarizing, optical data present that higher knock intensity can be correlated with higher in-cylinder pressure while pressure waves affect the residence time in the post flame region.

The observation of **Figure *12*** explains the 'right' limit region on **Figure *11***. NO formation depends on oxygen availability, peak temperature and the residence time of the mixture at high temperature conditions. In stoichiometric mixtures and under knocking conditions there is a competition between maximum cylinder temperature and residence time of combustion products in the burned region. As KI is increased, knock occurs earlier during the combustion process which means that residence time can potentially decrease although peak temperature and pressure are significantly enhanced. The latter affects the kinetic rate of NO formation and lead to lower emissions. In this study was found that combustion cycles with KI higher than 6 present a drop on NO emissions.

3.2 Effect of Air/Fuel Equivalence Ratio

Combustion evolution and knock onset are affected by mixture composition and oxygen availability, while fluctuations of air/fuel ratio is an important source of CCV [51]. Pollutants formation is also expected to be affected by the nature of the combustion and the oxygen availability.

The effect of oxygen availability on knock onset and pressure evolution is illustrated on **Figure *13*** that shows the in-cylinder pressure traces for three different mixtures: slightly rich, slightly lean and (almost) stoichiometric. The three (3) cycles correspond to identical ignition timing (20° BTDC), engine load (imep~4.4 bar) but different knock intensity conditions. It is observed that slightly rich mixture presents a faster burn rate and reaches end-gas auto-ignition limit closer to TDC, as due to the smaller cylinder volume of the unburned region, the unburned temperature and pressure are relatively high at this crank angle. On the other hand, slightly lean mixture is characterized by a slower burn rate and compared to the stoichiometric combustion cycle, the onset of knock at lean conditions appears with 5° CA delay.

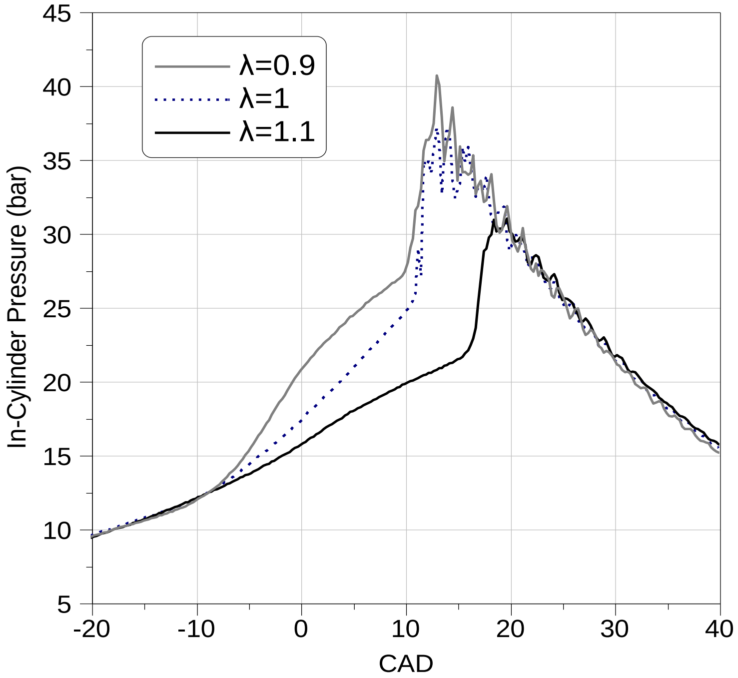

Figure 13: In-cylinder pressure traces for three (3) different air/fuel equivalence ratios and similar ignition timings (TDC-20°) and imep. Equivalence ratio significantly affects knock onset and peak in-cylinder pressure.

The knock resistance of lean mixtures has been investigated in the past by Gruden and Hahn [52]. In their study, a production engine was converted to a lean burn engine. Researchers explored the effect of many parameters on engine economy including: high compression ratio, optimization of ignition timing and layout of the combustion chamber shape with intensive charge turbulence. They found that compression ratio can be increased with lean operation, implying that lean mixtures are more knock resistant. However, the operating conditions under which this trend is valid is not clearly stated. Considering the results of **Figure *13***, a possible reason could be the slower burn rate that leads to auto-ignition when piston expands and consequently end gas temperature and pressure are relatively low.

In order to better understand the effect of air/fuel equivalence ratio on knock intensity and NO emissions, the 20^o BTDC ignition point was selected from stoichiometric data previously presented and experiments were performed for various air/fuel equivalence ratios. **Figure *14*** shows that maximum KI is observed at close to stoichiometric conditions, while under slightly lean conditions KI drops impressively. Conversely to previous studies where it was found that lean mixtures increase the COV of imep and cyclic combustion variability is much higher, knocking combustion lean mixtures reduce cyclic variability as KI drops. The effect of air/fuel equivalence ratio on NO formation under knocking combustion is also explored. It was found that maximum NO emissions are enhanced under lean conditions due to the excess of oxygen and the peak temperature conditions that occur under slightly lean conditions. Compared to normal combustion lean operating (λ~1.1) conditions, it was found that NO can be up to 3 times higher under autoignition conditions.

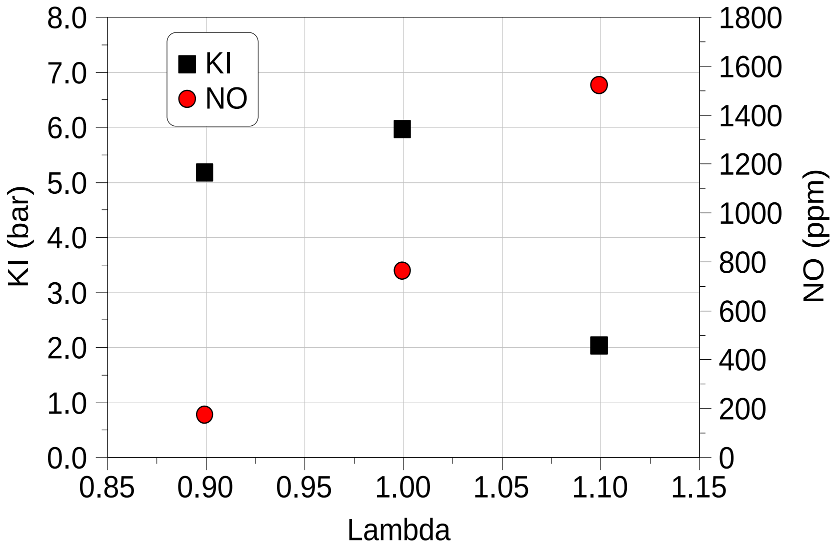

Figure 14: Effect of air/fuel ratio (λ) on average knock intensity and NO emissions for similar ignition timings (TDC-20) and engine load (imep~4.4 bar).

Cyclic combustion variability consists of both stochastic and deterministic phenomena [22]. Fluctuations of the gas mixture motion and turbulence and variation of the quantity and spatial distribution of the fuel are related with the stochastic aspect of cyclic dispersion. Leaner and more dilute mixture conditions are related to the deterministic aspect of cyclic variability [53] and can also affect the amplitude of knock intensity under knocking conditions. The latter is further discussed in this study.

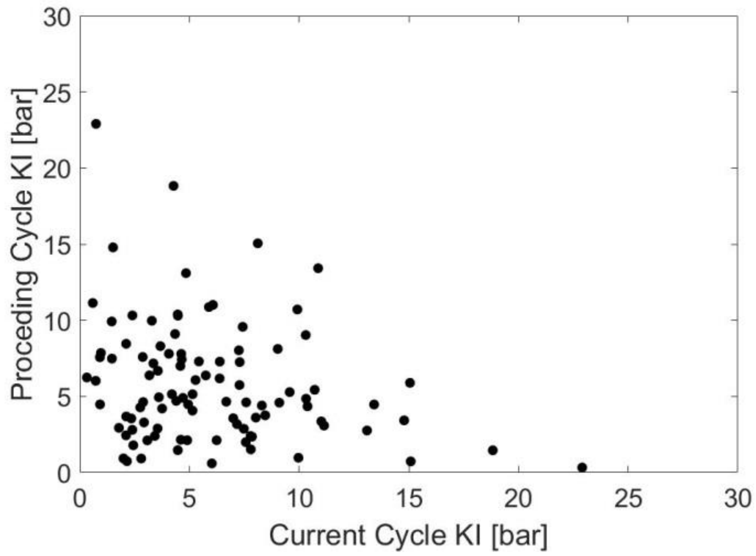

Figure 15: KI return map for ignition timing TDC-20 and stoichiometric air/fuel ratio conditions.

The return map is identified as an easy and fast way to characterize the nature of the variability of any index and it includes the plot of the current value against the previous or next cycle value of the same index. A boomerang-shaped pattern declares the deterministic aspect of variability while a noisy spot point shows the stochastic feature of the variability.

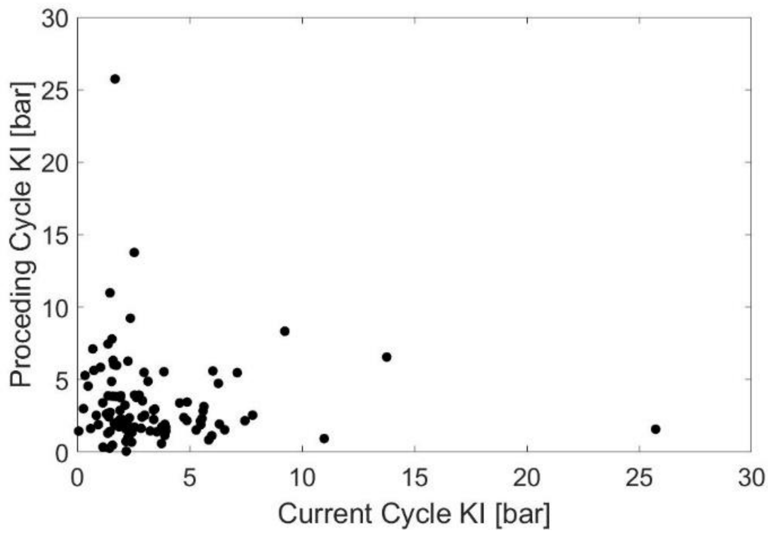

Figure 16: KI return map for ignition timing TDC-20 and slightly rich air/fuel ratio conditions.

Figure *15* and **Figure *16*** show the KI return map for stoichiometric and rich operating conditions respectively. It is observed that under stoichiometric conditions KI presents a boomerang-shaped pattern (**Figure *15***), while the scatter of data under rich conditions has been decreased in an almost noisy spot (**Figure *16***). This strong indication proves the deterministic character of knock intensity can significantly be reduced under rich conditions. The reason can be the well-known cooling effect of rich mixtures, that decreases the end-gas temperature and pressure and finally the knock intensity is reduced. It has to be noted that the small impact of mixture air/fuel equivalence ratio on average engine load (imep), which differs by 2% between the stoichiometric and rich mixtures, slightly affects the residual gas fraction, which is a strong deterministic combustion parameter.

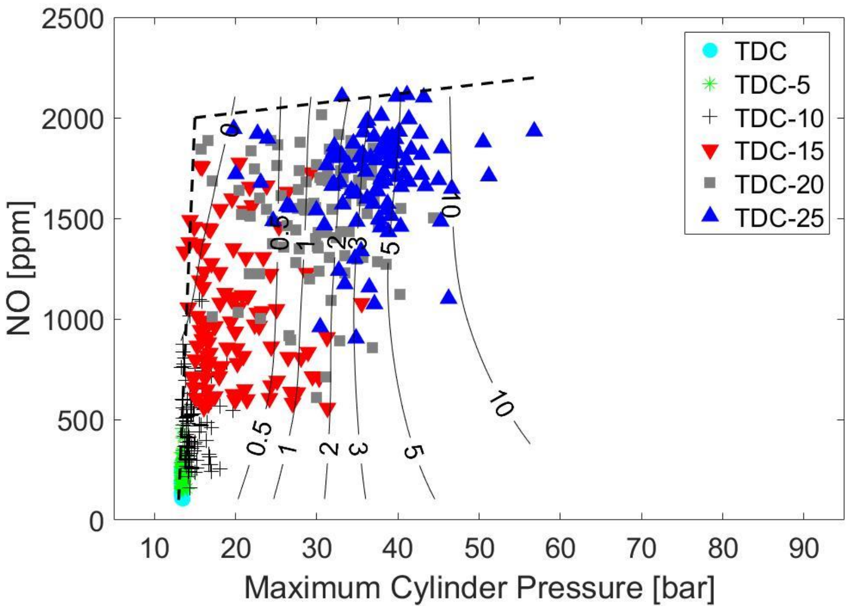

Figure 17: Relationship between maximum cylinder pressure and NO formation for various KI conditions (contour lines) as a result of various ignition timing conditions under slightly lean conditions (λ~1.1).

Nitric oxide formation is related with peak combustion temperature, mixture residence time at high temperature and oxygen availability [43]. A recent study proved that under normal combustion conditions, as a result of cyclic emission variability, fast burn rate cycles present peak formed NO emissions under slightly lean conditions while slow burn rate cycles present peak NO emissions closer to equivalent air/fuel ratio at unity [21].

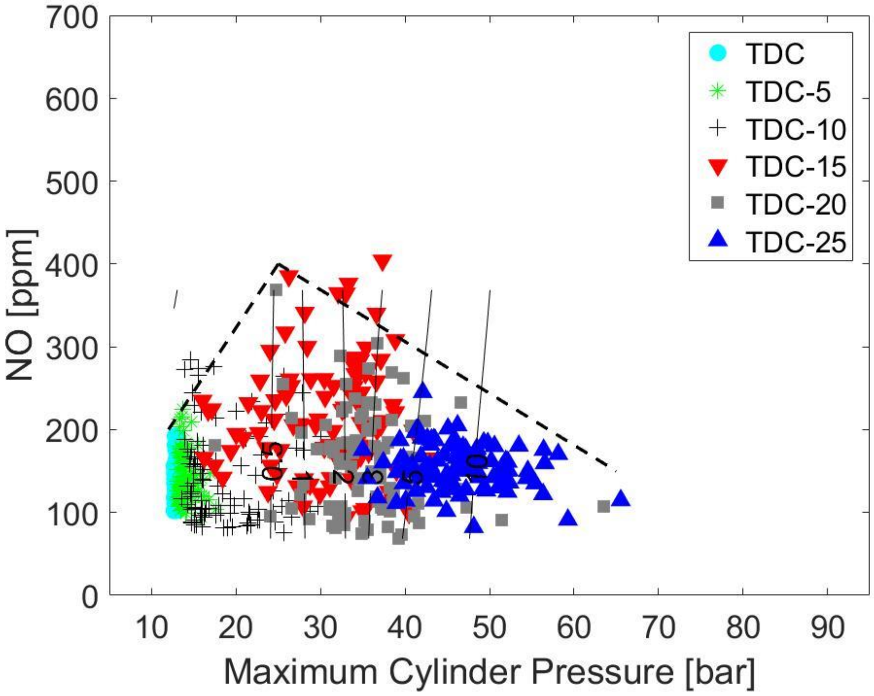

Figure 18: Relationship between maximum cylinder pressure and NO formation for various KI conditions (contour lines) as a result of various ignition timing conditions under slightly rich conditions (λ~0.9).

Under knocking combustion conditions, where peak temperatures are observed, oxygen availability seems to be the most important parameter for NO formation. **Figure *17*** illustrates the relationship between maximum in-cylinder pressure and NO formation for slight lean mixtures and various KI conditions, which are presented as contour lines in the plot. Similar to stoichiometric conditions presented before, the scatter area of the data form a triangular. The left limit matches with the KI=0 isoline; under normal combustion conditions NO is proportional to maximum in-cylinder pressure. Compared to stoichiometric conditions, the rate is much faster due to the excess of oxygen.

Although the ‘left’ limit at **Figure *17*** is similar to the trend found at **Figure *11***, the ‘right’ limit line is significantly different to stoichiometric conditions. The only parameter that alters between those figures is oxygen availability. The competitive relationship between peak temperature and residence time that was found under stoichiometric conditions is not appeared under slightly lean conditions. The excess oxygen enhances post flame NO kinetics which are further benefit from higher peak temperatures in high knock intensity combustion cycles. The general trend shows that under high KI values, NO emissions are clearly increased with the scatter of the data being also decreased, which means that the average value of NO follows an important increment.

On the opposite site, **Figure *18*** presents the relationship between maximum in-cylinder pressure and NO formation for slight rich mixtures and various KI conditions. The trends are identical to the previous discussed under stoichiometric conditions at **Figure *11***, presenting the competition between residence time and peak temperature for various KI conditions.

4 Conclusions

This study explores pollutants formation under knocking combustion conditions using an optical single cylinder SI engine. A novel experimental setup has been utilized including fast response analyzers for NO and HC emissions, natural light photography and in-cylinder pressure recordings. The effect of two engine operating parameters where explored such as spark ignition timing and air/fuel equivalence ratio.

The effect of ignition timing on pollutants formation under various knock index conditions has been explored. It was found that as spark timing is advanced and knock intensity is increased, both NO and HC emissions are enhanced. Up to knock intensity equal to 6 bar and under stoichiometric conditions, it was found that instantaneous NO emissions are increased by up to 60% compared to the MBT operating conditions. A further increase of knock intensity at the limits of pre-ignition region was found to significantly drop NO emissions. Simultaneously HC emissions were found to increase at the region of light and medium knock where the peak of HC emissions was observed, while at heavier knock region HC emissions drop.

The effect of air/fuel equivalence ratio on pollutants formation under knocking combustion has been also investigated in this study. It was found that leaner mixtures present the onset of knock later compared to richer mixtures due to the slower deflagration rate. When knock occurs, the formed NO in lean mixtures are higher than in stoichiometric or rich mixtures due to the oxygen availability. Last but not least, it was found that under lean conditions NO emissions are enhanced as knock intensity is increased while under stoichiometric or slightly rich operating conditions it was found that NO are decreased for knock intensity higher than 6 bar.

Acknowledgement

The authors would like to thank the personnel of the Centre of Advanced Powertrain and Fuels (CAPF) at Brunel University London for their support in the experimental part of this work.

References

[1] T. Johnson and A. Joshi, "Review of Vehicle Engine Efficiency and Emissions," in *SAE Technical Paper, 2018-01-0329*, 2018.

[2] G. C. Koltsakis, Z. Samaras, A. Karvountzis-Kontakiotis, T. Zacharopoulou, and O. Haralampous, "Implications of Engine Start-Stop on After-Treatment Operation," *SAE Int. J. Engines*, vol. 4, no. 1, 2011.

[3] Z. Wang, H. Liu, and R. D. Reitz, "Knocking combustion in spark-ignition engines," *Prog. Energy Combust. Sci.*, vol. 61, pp. 78–112, 2017.

[4] G. G. Zhu, C. F. Daniels, and J. Winkelman, "MBT Timing Detection and its Closed-Loop Control Using In-Cylinder," in *SAE Technical Paper*, 2003, no. 2003-01-3266.

[5] S. Diana, V. Giglio, B. Iorio, and G. Police, "A Strategy to Improve the Efficiency of Stoichiometric Spark Ignition Engines," in *SAE Technical Paper*, 1996.

[6] M. D. Gerty and J. B. Heywood, "An Investigation of Gasoline Engine Knock Limited Performance and the Effects of Hydrogen Enhancement," *SAE Tech. Pap.*, no. 2006-1–228, pp. 1–21, 2006.

[7] Z. Wang, Y. Qi, X. He, J. Wang, S. Shuai, and C. K. Law, "Analysis of pre-ignition to super-knock: Hotspot-induced deflagration to detonation," *Fuel*, vol. 144, pp. 222–227, 2015.

[8] G. T. Kalghatgi and D. Bradley, "Pre-ignition and 'super-knock' in turbo-charged spark-ignition engines," *Int. J. Engine Res.*, vol. 13, no. 4, pp. 399–414, Feb. 2012.

[9] X. Zhen *et al.*, "The engine knock analysis – An overview," *Appl. Energy*, vol. 92, pp. 628–636, 2012.

[10] X. Duan *et al.*, "Performance, combustion and knock assessment of a high

compression ratio and lean-burn heavy-duty spark-ignition engine fuelled with n-butane and liquefied methane gas blend," *Energy*, 2018.

[11] J. H. Mack, V. H. Rapp, M. Broeckelmann, T. S. Lee, and R. W. Dibble, "Investigation of biofuels from microorganism metabolism for use as anti-knock additives," *Fuel*, vol. 117, pp. 939–943, 2014.

[12] H. Vafamehr, A. Cairns, O. Sampson, and M. M. Koupaie, "The competing chemical and physical effects of transient fuel enrichment on heavy knock in an optical spark ignition engine," *Appl. Energy*, vol. 179, pp. 687–697, 2016.

[13] S. Diana, V. Giglio, B. Iorio, and G. Police, "Evaluation of the Effect of EGR on Engine Knock," *SAE Tech. Pap.*, no. 724, p. 982479, 1998.

[14] K. Kumano and S. Yamaoka, "Analysis of knocking suppression effect of cooled EGR in turbo-charged gasoline engine," *SAE Tech. Pap.*, no. 2014-01-1217, 2014.

[15] D. Song *et al.*, "Low Pressure Cooled EGR for Improved Fuel Economy on a Turbocharged PFI Gasoline Engine," *SAE Tech. Pap. 2014-01-1240*, 2014.

[16] T. Alger, T. Chauvet, and Z. Dimitrova, "Synergies between High EGR Operation and GDI Systems," *SAE Int. J. Engines*, vol. 1, no. 1, pp. 2008-01–0134, 2008.

[17] A. Cairns, H. Blaxill, and G. Irlam, "Exhaust Gas Recirculation for Improved Part and Full Load Fuel Economy in a Turbocharged Gasoline Engine," *SAE Tech. Pap.*, no. 724, 2006.

[18] H. Vafamehr, A. Cairns, and M. Moslemin Koupaie, "The Competing Chemical and Physical Effects of Transient Fuel Enrichment during Heavy Knock in an Optical SI Engine Using Ethanol Blends," *SAE Tech. Pap.*, vol. 2017–March, no. March, 2017.

[19] B. Grandin and H.-E. Ångström, "Replacing Fuel Enrichment in a Turbo Charged SI Engine: Lean Burn or Cooled EGR," *SAE Tech. Pap.*, vol. 1999-01-35, no. 724, 1999.

[20] B. Grandin, I. Denbratt, J. Bood, and C. Brackmann, "Heat Release in the End-Gas Prior to Knock in Lean, Rich and Stoichiometric Mixtures With and Without EGR," *SAE Tech. Pap.*, vol. 2002-1–2, 2002.

[21] A. Karvountzis-Kontakiotis, L. Ntziachristos, Z. Samaras, A. Dimaratos, and M. Peckham, “Experimental Investigation of Cyclic Variability on Combustion and Emissions of a High-Speed SI Engine,” *SAE Tech. Pap.*, vol. 2015–April, no. April, 2015.

[22] A. Karvountzis-Kontakiotis, A. Dimaratos, L. Ntziachristos, and Z. Samaras, “Exploring the stochastic and deterministic aspects of cyclic emission variability on a high speed spark-ignition engine,” *Energy*, vol. 118, 2017.

[23] J. K. Ball, M. J. Bowe, R. Stong, and N. Collings, “Validation of a Cyclic NO Formation Model with Fast NO Measurements,” in *SAE Technical Paper*, 2001, vol. 2001-01-10.

[24] N. P. Komninos and D. T. Hountalas, “Improvement and validation of a multi-zone model for HCCI engine combustion concerning performance and emissions,” *Energy Convers. Manag.*, vol. 49, no. 10, pp. 2530–2537, 2008.

[25] A. Karvountzis-Kontakiotis, “Impact of the Cycle-to-Cycle Variation of an Internal Combustion Engine to Gaseous Pollutants Emissions,” PhD Thesis, Aristotle University of Thessaloniki, 2015.

[26] G. A. Lavoie, J. B. Heywood, and J. C. Keck, “Experimental and Theoretical Study of Nitric Oxide Formation in Internal Combustion Engines,” *Combust. Sci. Technol.*, vol. 1, no. 4, pp. 313–326, Feb. 1970.

[27] C. T. Bowman, “Kinetics of pollutant formation and destruction in combustion,” *Prog. Energy Combust. Sci.*, vol. 1, no. 1, pp. 33–45, 1975.

[28] C. P. Fenimore, “Formation of nitric oxide in premixed hydrocarbon flames,” *Symp. Combust.*, vol. 13, no. 1, pp. 373–380, 1971.

[29] J. A. Miller and C. T. Bowman, “Mechanism and modeling of nitrogen chemistry in combustion,” *Prog. Energy Combust. Sci.*, vol. 15, no. 4, pp. 287–338, 1989.

[30] F. BACHMAIER, K. H. EBERIUS, and T. H. JUST, “The Formation of Nitric Oxide and the Detection of HCN in Premixed Hydrocarbon-Air Flames at 1 Atmosphere,” *Combust. Sci. Technol.*, vol. 7, no. 2, pp. 77–84, Apr. 1973.

[31] J. W. Bozzelli and A. M. Dean, "O + NNH: A possible new route for NOX formation in flames," *Int. J. Chem. Kinet.*, vol. 27, no. 11, pp. 1097–1109, 1995.

[32] S. Javoy, R. Mevel, and C. E. Paillard, "A study of N2O decomposition rate constant at high temperature: Application to the reduction of nitrous oxide by hydrogen," *Int. J. Chem. Kinet.*, vol. 41, no. 5, pp. 357–375, 2009.

[33] G. D'Errico, G. Ferrari, A. Onorati, and T. Cerri, "Modeling the Pollutant Emissions from a S.I. Engine," *SAE Tech. Pap.*, vol. 2002-01–00, 2002.

[34] G. Merker, C. Schwarz, G. Stiesch, and F. Otto, *Simulation of combustion and pollutant formation for engine-development*. Springer-Verlag Berlin Heidelberg, 2006.

[35] M. Rublewski and J. Heywood, "Modeling NO Formation in Spark Ignition Engines with a Layered Adiabatic Core and Combustion Inefficiency Routine," *SAE Tech. Pap.*, vol. 2001-01-10, 2001.

[36] A. T. Karvountzis-Kontakiotis and L. Ntziachristos, "A detailed chemical mechanism to predict NO Cycle-to-cycle Variation in homogeneous engine combustion," in *IFAC Proceedings Volumes (IFAC-PapersOnline)*, 2012.

[37] A. Karvountzis-Kontakiotis and L. Ntziachristos, "Investigation of cycle-to-cycle variability of NO in homogeneous combustion," *Oil Gas Sci. Technol.*, vol. 70, no. 1, 2015.

[38] A. Karvountzis-Kontakiotis and L. Ntziachristos, "Improvement of NO and CO predictions for a homogeneous combustion SI engine using a novel emissions model," *Appl. Energy*, vol. 162, 2016.

[39] W. E. Holly, T. Lauer, H. A. Schuemie, and S. Murakami, "Prediction of the knocking combustion and NOx formation for fuel gases with different methane numbers," *Int. J. Engine Res.*, vol. 17, no. 1, pp. 35–43, Dec. 2015.

[40] S. Richard, S. Bougrine, G. Font, F.-A. Lafossas, and F. Le Berr, "On the Reduction of a 3D CFD Combustion Model to Build a Physical 0D Model for Simulating Heat Release, Knock and Pollutants in SI Engines," *Oil Gas Sci. Technol. - Rev. IFP*, vol. 64, no. 3, pp. 223–242, 2009.

[41] C. D. Rakopoulos and C. N. Michos, “Development and validation of a multi-zone combustion model for performance and nitric oxide formation in syngas fueled spark ignition engine,” *Energy Convers. Manag.*, vol. 49, no. 10, pp. 2924–2938, 2008.

[42] Y. Zhuang, Y. Qian, and G. Hong, “The effect of ethanol direct injection on knock mitigation in a gasoline port injection engine,” *Fuel*, vol. 210, pp. 187–197, 2017.

[43] A. Karvountzis-Kontakiotis, A. Dimaratos, L. Ntziachristos, and Z. Samaras, “Exploring the stochastic and deterministic aspects of cyclic emission variability on a high speed spark-ignition engine,” *Energy*, vol. 118, pp. 68–76, 2017.

[44] H. Zhao, *Laser Diagnostics and Optical Measurement Techniques in Internal Combustion Engines*. SAE International, 2012.

[45] S. Dingle, A. Cairns, H. Zhao, and J. Williams, “Lubricant Induced Pre-Ignition in an Optical SI Engine,” *SAE Tech. Pap.*, vol. 2014-01-12, 2014.

[46] T. Goto, R. Isobe, M. Yamakawa, and M. Nishida, “The New Mazda Gasoline Engine Skyactiv-G,” *ATZ Auto-Technol*, vol. 11:40–7, 2011.

[47] J. Heywood, *Internal Combustion Engine Fundamentals*. New York: McGraw-Hill, 1988.

[48] M. Peckham, A. Finch, and B. Campbell, “Analysis of Transient HC, CO, NOx and CO2 Emissions from a GDI Engine using Fast Response Gas Analyzers,” *SAE Int. J. Engines*, vol. 4, no. 1, 2011.

[49] K. S. J. Reavell, N. Collings, M. Peckham, and T. Hands, “Simultaneous Fast Response NO and HC Measurements from a Spark Ignition Engine,” *SAE Tech. Pap.*, vol. 971610, no. 412, 1997.

[50] J. K. Ball, R. R. Raine, and C. R. Stone, “Combustion analysis and cycle-by-cycle variations in spark ignition engine combustion Part 2: a new parameter for completeness of combustion and its use in modelling cycle-by-cycle variations in combustion,” *Proc. Inst. Mech. Eng. Part D J. Automob. Eng.*, vol. 212, no. 6, pp. 507–523, 2005.

[51] G. Grünefeld, V. Beushausen, P. Andresen, and W. Hentschel, “A Major Origin of

Cyclic Energy Conversion Variations in SI Engines: Cycle-by-Cycle Variations of the Equivalence Ratio and Residual Gas of the Initial Charge,” *SAE Tech. Pap.*, vol. 941880, 1994.

[52] D. Gruden and R. Hahn, “Performance, exhaust emissions and fuel consumption of an IC engine operating with lean mixtures,” in *IMechE Conference on Fuel Economy and Emissions of Lean Burn Engines, C111/79*, 1979, pp. 177–184.

[53] C. E. A. Finney, B. C. Kaul, C. S. Daw, R. M. Wagner, K. D. Edwards, and J. B. Green, “Invited Review: A review of deterministic effects in cyclic variability of internal combustion engines,” *Int. J. Engine Res.*, vol. 16, no. 3, pp. 366–378, Feb. 2015.